

Photoconductivity of Pea-Pod-Type Chains of Gold Nanoparticles Encapsulated within Dielectric Amyloid Protein Nanofibrils of α -Synuclein**

Daekyun Lee, Young-Jun Choe, Yeon Sun Choi, Ghibom Bhak, Jihwa Lee, and Seung R. Paik*

Encapsulation of noble-metal nanoparticles within dielectric matrices has been used to develop fast optoelectric response systems near the surface plasmon resonance (SPR) frequency.^[1] Light energy can thus be transported through nanoparticles whose sizes are substantially smaller than the wavelength of corresponding light.^[2] We introduce herein a convenient bottom-up approach to fabricate a pea-pod-type gold-nanoparticle (AuNP) arrangement into anisotropic one-dimensional chain structures within the dielectric amyloid fibrils of α -synuclein. The assembly units composed of α -synuclein encapsulating AuNPs were manipulated by either hexane or the pH value to induce structural rearrangement within the protein coat. These structural alterations led to instantaneous AuNP alignment into the pea-pod-type chain structures from single- to multichain format wrapped with the fibrillar protein coat. These AuNP-embedded amyloid protein nanofibrils exhibited photoconductivity with visible light; this property is essential for the development of a subwavelength-size light-guiding system that could contribute to the continuous pursuit of miniaturization of nanooptics.^[3] Our approach, therefore, offers a facile and general means to align noble-metal nanoparticles into chain structures. Moreover, the properties of insulation, rich chemistry for modification, and biocompatibility provided by the protein sheath make the resulting nanochains multifunctional photoconductive fusion nanomaterials that are suitable for applications in future nano-biotechnology applications.


Nanoparticles of metals, semiconductors, and oxides exhibit well-defined nanoscale properties, such as electrical, optical, magnetic, and catalytic properties, which have been improved by altering their size, shape, and composition.^[4] Their realm of usefulness can be increased by harnessing interparticle properties.^[5] Assembly of nanoparticles into desired and controllable nanoobjects, therefore, is a crucial

task to raise their application potential for the development of nanoscale electronic and optical devices.^[6,7] Among methods to arrange nanoparticles into functional geometries, biopolymers have provided effective and reliable means for organizing nanoparticles into suprastructures. For example, double-stranded DNA chains and protein/peptide-based supramolecular structures such as microtubules and amyloid fibrils could provide templates for the assembly of inorganic nanoparticles to produce nanowires.^[8] DNA hybridization and actin polymerization could be also utilized for the control of nanoparticle assembly.^[9]

In particular, fabrication of anisotropic one-dimensional noble-metal nanoparticle chains to obtain integrated optics operating below the diffraction limit of light has garnered much attention.^[2,10,11] In fact, numerous efforts have been made to embed noble-metal nanoparticles within dielectric matrixes in high density by employing sol-gel processes, metal-ion implantation, and metal sputtering.^[12–14] Herein, we introduce a convenient bottom-up strategy to assemble AuNPs into the one-dimensional chain structures within a dielectric protein matrix of amyloid fibrils. This novel pea-pod-type AuNP alignment, therefore, could satisfy the demand of developing nanoscale optoelectric systems exhibiting photoconductivity operated with visible light. Amyloid fibrils have been intensely investigated because of their pathological implications to various neurodegenerative disorders, such as Parkinson's and Alzheimer's diseases.^[15–17] Those protein nanofibrils have also been suggested to be applied in various areas including conductive nanowire preparation, nanomatrix production for applications such as drug deposition and cell growth, and liquid-crystal formation.^[18] In particular, their mechanical strength was reported to be comparable to that of spider silk.^[19] Recently, we demonstrated that amyloid fibrils of α -synuclein, a pathological component of Parkinson's disease by participating in the Lewy body formation as the major constituent, could be generated through a unit assembly process of the preformed oligomeric granular species of α -synuclein.^[20,21] Following subtle structural rearrangement of the oligomers with physical or chemical influences such as shear stress and hexane treatment, the fibrillation was dramatically accelerated. Depending on fibrillation processes, the amyloid fibrils exhibited morphological polymorphism to produce either curly or straight amyloid fibrils from a single protein of α -synuclein; it was the curly fibrils that turned into the amyloid hydrogel.^[22] This novel mechanism has been acknowledged by naming it as double-concerted fibrillation

[*] Dr. D. Lee, Dr. Y.-J. Choe, Y. S. Choi, G. Bhak, Prof. J. Lee, Prof. S. R. Paik
School of Chemical and Biological Engineering
College of Engineering, Seoul National University
Seoul 151-744 (Korea)
E-mail: srpaik@snu.ac.kr
Homepage: <http://plaza.snu.ac.kr/~apml/>

[**] This research was supported by the Korea Healthcare Technology R&D Project (A08-A217-08N1-00010A) of Ministry for Health, Welfare, and Family Affairs.

 Supporting information for this article (details of all experimental procedures) is available on the WWW under <http://dx.doi.org/10.1002/anie.201004301>.

to parallel the prevalent mechanism of nucleation-dependent fibrillation.^[20,23]

In this study, therefore, the unit assembly strategy of amyloid fibril formation of α -synuclein was employed to construct anisotropic one-dimensional chains of AuNPs within the amyloid protein fibrils. As depicted in Figure 1,

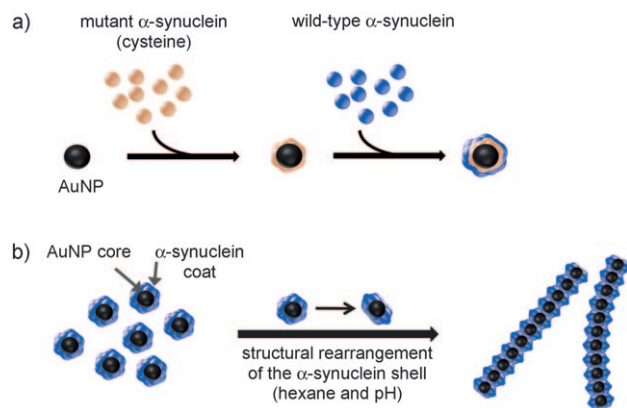


Figure 1. a) Double-layer coating of AuNPs with the α -synucleins of cysteine-incorporated mutant and wild-type form; b) alignment of AuNPs into amyloid fibrils of α -synuclein by treatment with hexane or a pH change.

AuNPs must be coated with α -synuclein prior to their structural rearrangement caused by either hexane or a pH change for the formation of the nanoparticle-containing protein fibril. AuNPs were coated with α -synuclein in a double layer (Figure 1a). The first layer was prepared with mutant α -synuclein containing a single cysteine residue to covalently attach the protein to the AuNP surface. Subsequently, the second layer was added, consisting of wild-type α -synuclein to transpose its inherent self-assembly properties to the assembly unit. Since wild-type α -synuclein has no cysteine residue in its primary structure, site-directed mutagenesis was performed to have three separate mutant forms such as S9C, A53C, and Y136C by replacing each amino acid of Ser-9, Ala-53, and Tyr-136 with cysteine residues, respectively. All the AuNPs sheathed with the mutant α -synucleins showed no sign of flocculation in the presence of NaCl (see Figure S1 in the Supporting Information), confirming thiolate-mediated conjugation of the mutant α -synucleins to AuNPs. The first protein layer in the A53C-coated AuNP appeared in a transmission electron microscopy (TEM) image as a white corona surrounding the nanoparticle with an average thickness of (2.08 ± 0.43) nm (Figure 2a). The thickness increased up to (4.20 ± 0.35) nm (Figure 2a) as the A53C-conjugated AuNP (AuNP-A53C) was incubated with wild-type α -synuclein for two consecutive coating steps to allow the protein to experience the structural rearrangement essential for the unit assembly. Intriguingly, however, the other conjugates, AuNP-S9C and AuNP-Y136C, hardly increased the thickness of the second layer, which resulted in a thickness of entire protein coat of (2.87 ± 0.25) nm and (2.61 ± 0.36) nm, respectively (see Table S1 in the Supporting Information). These data might indicate that optimal protein–

protein interaction with wild-type α -synuclein was restricted for the mutant proteins of S9C and Y136C attached on AuNP by confining the N terminus and C terminus to the nanoparticle surface, respectively. Since precise self-assembly properties ought to be essential for the fibrillation of α -synuclein, α -synuclein interactive AuNP-A53C was chosen to induce the AuNP-containing protein nanofibril formation.

To engineer AuNPs into the anisotropic chain structure, a subtle structural rearrangement of the α -synuclein localized on AuNP was achieved by treating the assembly units with 5% hexane (Figure 1b), which was previously demonstrated to give rise to instantaneous fibrillation of the α -synuclein oligomeric granular species.^[21] Initially, the AuNPs coated with the first protein layer of A53C were examined to test our proposal. As expected, AuNPs were indeed aligned into the discrete pea-pod-type anisotropic chain structure wrapped with the dielectric protein with an average interparticle distance of (6.17 ± 0.52) nm (Figure 2b). When the AuNPs with double layer exposing wild-type α -synuclein on the surface were triggered to assemble with the organic solvent, the pea-pod-type single AuNP chain was elongated to μ m scale, although a few AuNPs were missing in the middle of the strand (Figure 2c). Since the noncovalently bound α -synuclein could also independently participate in the fibrillation, the unrestricted α -synuclein in the second layer would be responsible for losing the particles during the assembly process especially under the harsh incubation condition of using an organic solvent. The α -synuclein-coated AuNP units prepared with either S9C or Y136C, however, failed to form the chain structures in the presence of hexane (data not shown), indicating that the specific protein–protein interaction observed with A53C and wild-type α -synuclein on the surface of AuNP is crucial for the unit-assembly process. In addition, the immediate alignment of the A53C-coated AuNP was considered to require simultaneous association of those structurally affected AuNP-containing units in the presence of the organic solvent, since the α -synuclein-AuNP units could not extend the preformed amyloid fibrils prepared without AuNP when they were treated together with 5% hexane. Instead, those particles sporadically attached to side surfaces of the pre-existing amyloid fibrils (see Figure S2 in the Supporting Information).

To reveal molecular assembly of the protein operating in the region between AuNPs within the chains, two representative assays of congo red birefringence and thioflavin-T binding fluorescence, which have been frequently used to define amyloid fibril formation, were performed. Normal amyloid fibrils of α -synuclein without the AuNPs embedded clearly showed apple-green birefringence from the congo red dyes intercalated regularly into the ordered molecular structures within the fibrils (Figure 2d). In contrast, bare AuNPs and the AuNPs coated with α -synuclein appeared red under the polarizer, indicating a lack of birefringence (Figure 2d). The AuNP-containing pea-pod type fibrils obtained with the hexane, however, showed the bright green birefringence upon the congo red binding, suggesting that the molecular assembly of α -synuclein observed in the normal amyloid fibril formation was indeed operative in the AuNP

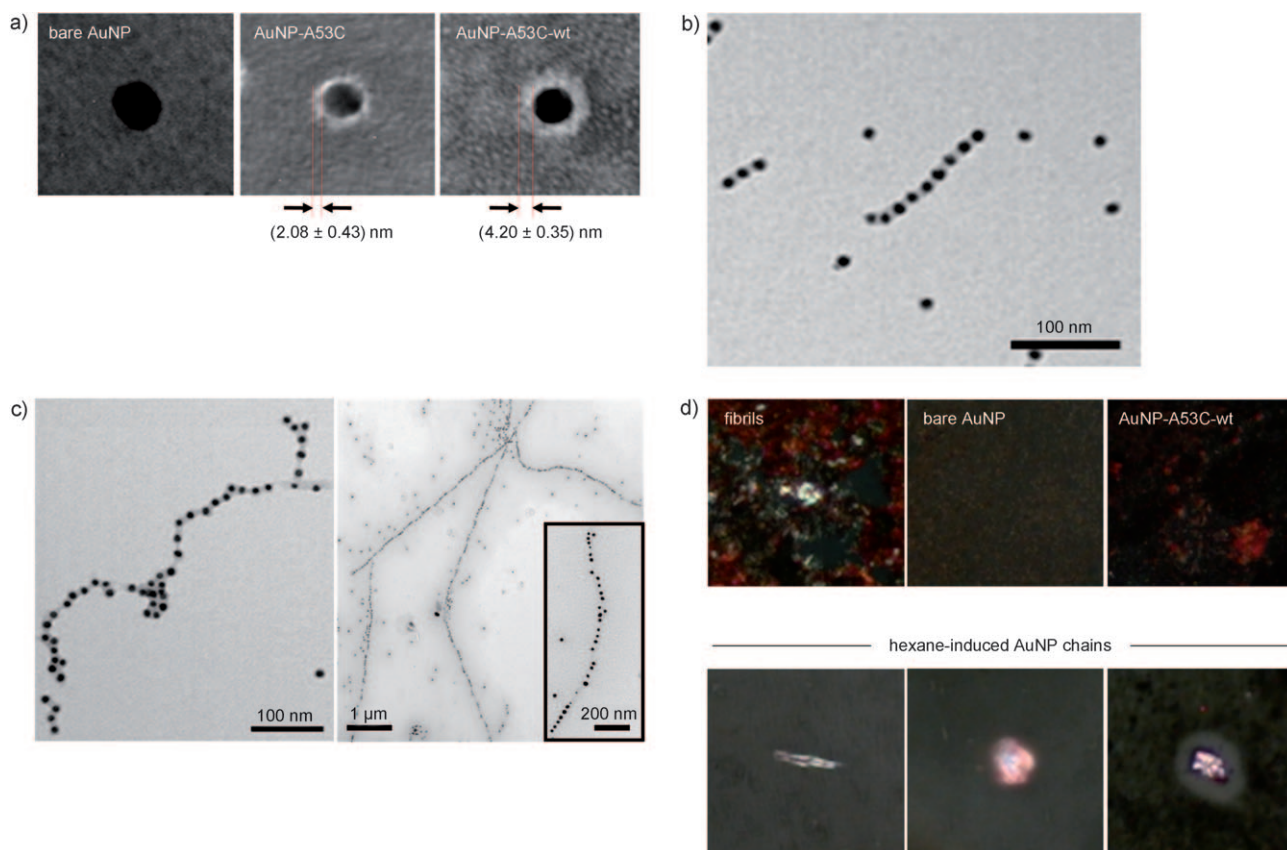


Figure 2. Thickness of the α -synuclein layer on AuNP and hexane-induced alignment of the α -synuclein-coated AuNPs into amyloid fibrils. a) TEM images of the α -synuclein layer on the AuNP surface. Covalently bound first layer of A53C (AuNP-A53C, middle) and the protein layer including the second layer of wild-type α -synuclein (AuNP-A53C-wt, right) are shown in negative stain with 2% uranyl acetate. Wild-type α -synuclein formed the second protein layer by incubation with AuNP-A53C at 37°C for 6 h with vigorous shaking. b,c) TEM images of chain structures of AuNP-A53C (b) and AuNP-A53C-wt (c) aligned with the 5% hexane treatment; inset: magnified image of a single AuNP chain. d) Congo red birefringence of the hexane-induced AuNP chains. With a polarizing microscope, the birefringence of the AuNP chains was revealed after staining with 1% saturated congo red (bottom panels). As controls, birefringence images of preformed amyloid fibrils of α -synuclein, bare AuNPs, and AuNP-A53C-wt without the hexane treatment are shown (upper panels).

assembly process (Figure 2d). In fact, thioflavin-T binding fluorescence of the AuNP-containing protein nanofibrils also became evident as the α -synuclein-coated AuNPs were aligned with the organic solvent (see Figure S3 in the Supporting Information). These data clearly indicate that the AuNP alignment was mediated by the ordered structure of β -sheet conformation between α -synuclein molecules, as typically found in normal amyloid fibrils, which could thus provide a formidable mechanical strength to the α -synuclein-mediated AuNP chains useful for future applications in nanobiotechnology.^[24]

We believe that our unit-assembly procedure might provide a facile and flexible strategy to embed various nanoparticles including AuNPs within the dielectric protein nanofibrils of α -synuclein in an anisotropic way. To improve AuNP alignment for their uniform distribution throughout the chains without the missing spots, milder conditions than the organic solvent treatment were required during the assembly of the particle-containing protein units. The chemical environment for the α -synuclein self-assembly could be carefully controlled by changing the pH value of the reaction medium. As the pH value was lowered to 4.2, which is slightly

more acidic than the isoelectric point of α -synuclein ($pI = 4.7$), AuNP-A53C particles with the second layer of wild-type α -synuclein were aligned into the pea-pod-type chain structures, whereas AuNP-A53C without the second layer unexpectedly failed to form the chains, indicating the importance of noncovalently attached wild-type α -synuclein and its structural rearrangement in the nanochain fabrication process. Unlike the hexane-induced nanochains, mostly generated as single-stranded AuNPs, however, the pH-induced AuNP chains consisted of double or multiple strands of the nanoparticles and extended over 10 μm in length (Figure 3a). In addition, AuNPs within the multichain configuration were revealed to be associated more tightly with an average interparticle distance of (2.02 ± 0.38) nm, which was decreased from that $((14.52 \pm 5.4)$ nm) of the hexane-induced chains by 85% (Figure 3b). These pH-induced AuNP chains also exhibited congo red birefringence (Figure 3c), as observed in both cases of normal amyloid fibril formation of α -synuclein and the hexane-induced AuNP chain formation. As AuNPs were aligned into the multichain structures, the UV/visible absorption maximum due to the surface plasmon resonance (SPR) of AuNPs was shifted to $\lambda =$

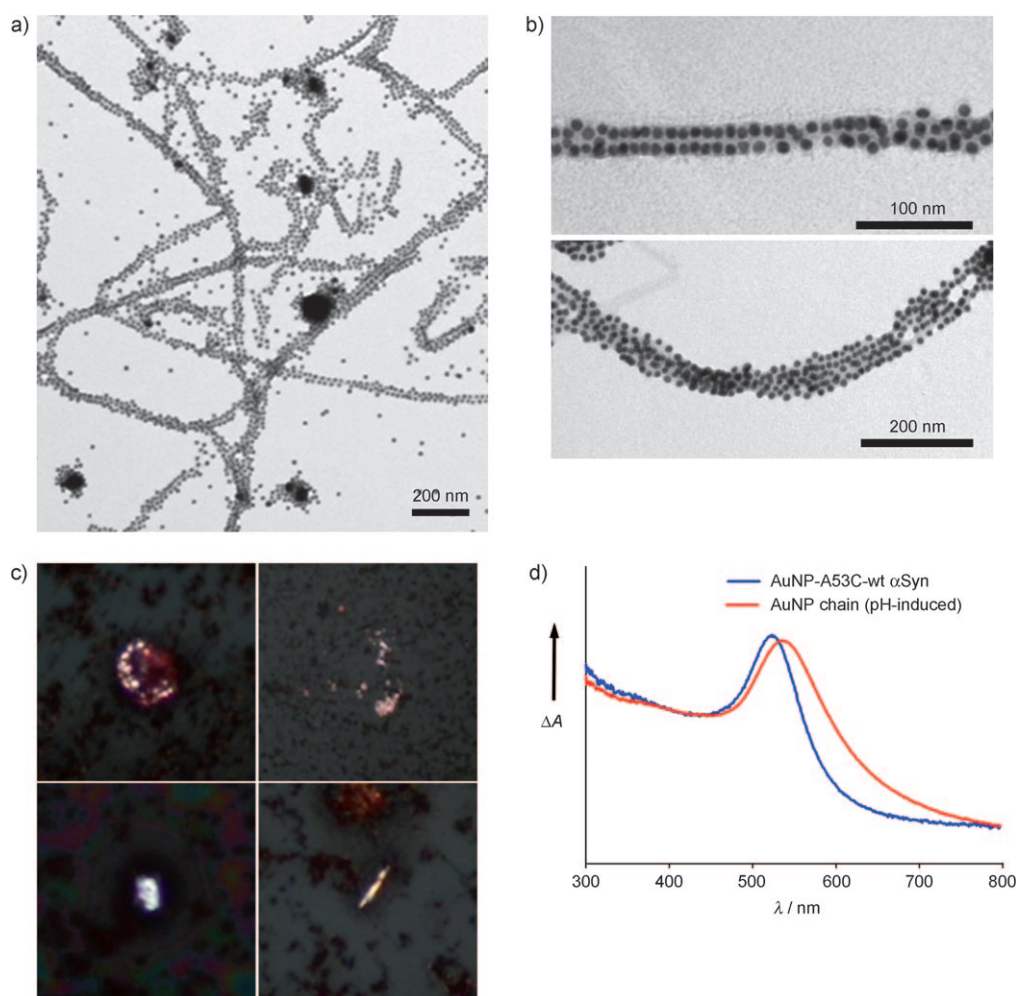


Figure 3. pH-induced AuNP nanochains embedded in α -synuclein amyloid fibrils. a) TEM image of the pH-induced AuNP chains prepared with AuNP-A53C-wt. The chains were derived by incubation of AuNP-A53C-wt in 10 mM citrate (pH 4.2) at 37°C for 1 h. b) Magnified images show double- (top) and multistranded chain structures (bottom) of AuNP. c) Congo red birefringence of the pH-induced AuNP chains. d) Surface plasmon resonance band of the pH-induced AuNP chains in comparison with monodisperse AuNP-A53C-wt.

537 nm from $\lambda = 523$ nm obtained with the unassembled AuNP-A53C- α -synuclein units (Figure 3d), indicating that the SPR bands of individual AuNPs were coupled within the chain structures. A low pH value was previously shown to augment the amyloid fibrillation of α -synuclein by minimizing large net negative charge of the protein.^[25] It was the alteration in surface charge of α -synuclein that would be responsible for formation of the long and compact multichain architecture of the AuNP-amyloid fibril hybrid chain structures.

These pea-pod-type anisotropic multichains of AuNP wrapped with the dielectric fibrils of α -synuclein were examined for their SPR-induced conductive effect by providing a subwavelength-size light-guiding system. Since those AuNP chains were prepared in multichain format, any missing AuNP could be complemented by the particles located on the adjacent chains, although missing particles were hardly found in these chain structures. Field-emission scanning electron microscopy (FE-SEM) verified adsorption of the hybrid nanochains on an oxidized silicon wafer with two electrodes

made of silver paste spaced 1 mm apart (Figure 4a). The AuNP chain structures, clearly revealed as multichain AuNP hybrid nanofibrils with an average width of 57.3 nm (Figure 4a, inset), were fully extended over 10 μ m in length and overlapped with one another to span the two electrodes. Two-terminal measurement of the current-voltage (I - V) characteristic demonstrated that the pH-induced AuNP multichain bundles prepared in a long-extended state with the closely spaced AuNPs embedded in the dielectric protein matrix were capable of conducting electricity even in the absence of catalytic enlargement with chloroauric acid.^[9b] The compact lateral association of AuNPs derived by the unit-assembly mechanism of α -synuclein fibrillation resulted in an interparticle distance close enough to transfer electrons through the dielectric matrix. I - V monitoring of the AuNP chains revealed a nonlinear I - V curve in which the current

increased linearly to the applied voltage only from 1.2 V after a nonresponding lag phase (Figure 4b). The AuNP-amyloid fibril hybrid chains required electrical stimulation before they became capable of conducting the current, which could be due to internal rearrangement of both AuNP and α -synuclein required for the conduction to occur. Neither bare silicon wafer nor normal amyloid fibrils of α -synuclein without AuNPs yielded any conductivity within this field intensity. Photoconductivity of the AuNPs encapsulated within the dielectric amyloid protein fibrils was examined by illuminating visible light with a solar simulator to the AuNP chains on the silica surface electrode under a constant electric field applied at 0.5 V. Conductivity of our hybrid AuNP-amyloid fibril chains quickly responded to the repetitive on-off irradiation cycle (Figure 4c). This result clearly demonstrates that the AuNPs aligned in multichains within the dielectric protein fibrils were able to mediate the transfer of electrons liberated by the enhanced third-order nonlinear susceptibility of AuNPs near their SPR frequency. In conclusion, we have successfully constructed anisotropic AuNP chains within a

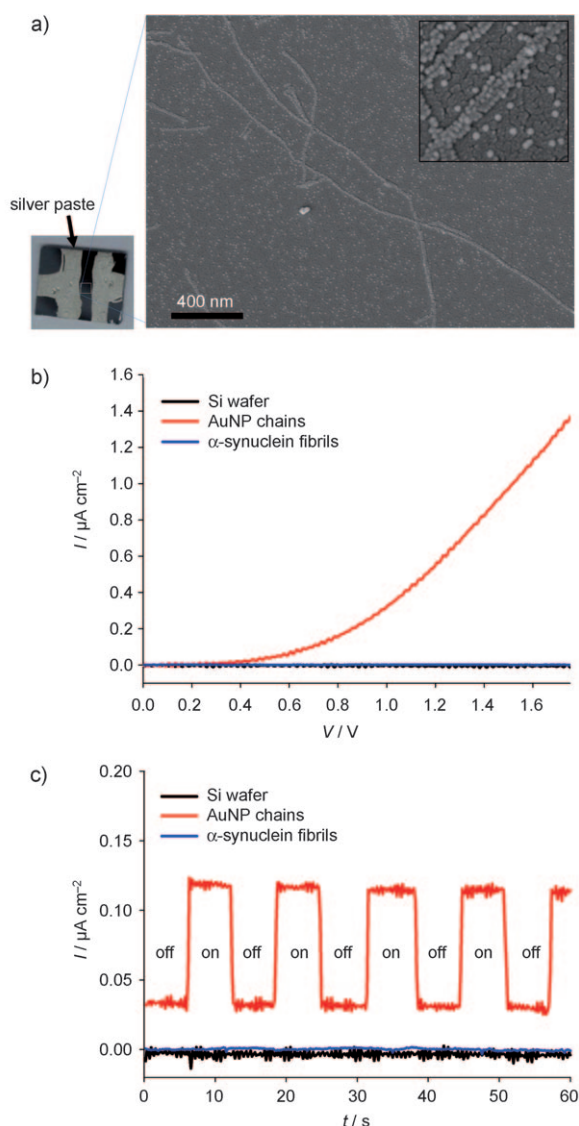


Figure 4. Electrical conductivity and photoconductivity of the pH-induced AuNP nanochains. a) SEM image of the pH-induced AuNP chains adsorbed on the surface of an oxidized Si wafer. The arrow indicates the silver paste acting as electrode for the conductivity measurement. The SEM image was obtained for the chains located between two silver electrodes. Inset: Magnified image of the pH-induced AuNP multichain structures. b) I - V curve obtained with the pH-induced AuNP chains deposited on the Si wafer. c) Periodic changes in current density of the pH-induced AuNP chains upon on/off cycling of the irradiation with a solar simulator in the presence of a constant voltage of 0.5 V. As a control, amyloid fibrils of α -synuclein without the embedded AuNPs were monitored for their intrinsic I - V characteristics and photoresponse.

dielectric protein matrix capable of exhibiting photoconductivity near the SPR frequency by taking advantage of molecular propensity of α -synuclein to form the protein fibrillar suprastructures and our newly discovered fibrillation mechanism of the unit-assembly process.^[20,21]

Our strategy employs a facile unit assembly procedure of novel self-interactive building blocks made of amyloidogenic α -synuclein encapsulating AuNP to construct the high-order nanostructures, representing a typical bottom-up approach to

fabricate a functional large structure of noble-metal nanoparticles. This procedure offers additional advantages over other embedding strategies using silica nanowire, mesoporous silica film, and polymer matrices.^[1,26,27] The high density of AuNPs aligned within the nanofibrils allows the optic response to be expressed with visible light under normal intensity without the need for a high-intensity laser beam for photostimulation. Other types of nanoparticles including magnetic, semiconductor, and fluorescent particles could also be linearly assembled within the protein matrix, which would further widen the scope of their applications. Since the dielectric matrix is made of the polypeptide α -synuclein, its biocompatibility affords hybrid nanobiomaterials for bio-machine interfaces. The polypeptide layer also offers additional functionalization owing to the rich chemistry of amino acids, which can be implemented in numerous areas by providing multifunctional photoconductive fusion materials useful for future nanobiotechnology including bioelectronics, chemical sensors, drug delivery, and tissue engineering.^[28]

Received: July 14, 2010

Revised: October 13, 2010

Published online: December 29, 2010

Keywords: fibrous proteins · gold · nanoparticles · photophysics · self-assembly

- [1] M. S. Hu, H. L. Chen, C. H. Shen, L. S. Hong, B. R. Huang, K. H. Chen, L. C. Chen, *Nat. Mater.* **2006**, 5, 102.
- [2] M. Quinten, A. Leitner, J. R. Krenn, F. R. Aussenegg, *Opt. Lett.* **1998**, 23, 1331.
- [3] S. A. Maier, P. G. Kik, H. A. Atwater, S. Meltzer, E. Harel, B. E. Koel, A. A. Requicha, *Nat. Mater.* **2003**, 2, 229.
- [4] H. Goesmann, C. Feldmann, *Angew. Chem.* **2010**, 122, 1402; *Angew. Chem. Int. Ed.* **2010**, 49, 1362.
- [5] S. Srivastava, N. A. Kotov, *Soft Matter* **2009**, 5, 1146.
- [6] S. I. Lim, C. J. Zhong, *Acc. Chem. Res.* **2009**, 42, 798.
- [7] Y. Ofir, B. Samanta, V. M. Rotello, *Chem. Soc. Rev.* **2008**, 37, 1814.
- [8] a) M. G. Warner, J. E. Hutchison, *Nat. Mater.* **2003**, 2, 272; b) G. Wang, R. W. Murray, *Nano Lett.* **2004**, 4, 95; c) J. C. Zhou, Y. Gao, A. A. Martinez-Molares, X. Jing, D. Yan, J. Lau, T. Hamasaki, C. S. Ozkan, M. Ozkan, E. Hu, B. Dunn, *Small* **2008**, 4, 1507; d) X. Fu, Y. Wang, L. Huang, Y. Sha, L. Gui, L. Lai, Y. Tang, *Adv. Mater.* **2003**, 15, 902.
- [9] a) A. G. Kanaras, Z. Wang, A. D. Bates, R. Cosstick, M. Brust, *Angew. Chem.* **2003**, 115, 201; *Angew. Chem. Int. Ed.* **2003**, 42, 191; b) F. Patolsky, Y. Weizmann, I. Willner, *Nat. Mater.* **2004**, 3, 692.
- [10] M. Brongersma, J. W. Hartman, H. A. Atwater, *Phys. Rev. B* **2000**, 62, R16356.
- [11] N. Sharma, A. Top, K. L. Kiick, D. J. Pochan, *Angew. Chem.* **2009**, 121, 7212; *Angew. Chem. Int. Ed.* **2009**, 48, 7078.
- [12] D. Dalacu, L. Martinu, *Appl. Phys. Lett.* **2000**, 77, 4283.
- [13] S. T. Selvan, T. Hayakawa, M. Nogami, Y. Kobayashi, L. M. Liz-Marzan, Y. Hamanaka, A. Nakamura, *J. Phys. Chem. B* **2002**, 106, 10157.
- [14] W. T. Wang, Z. H. Chen, G. Yang, D. Y. Guan, G. Z. Yang, Y. L. Zhou, H. B. Lu, *Appl. Phys. Lett.* **2003**, 83, 1983.
- [15] M. Bucciantini, E. Giannoni, F. Chiti, F. Baroni, L. Formigli, J. Zurdo, N. Taddei, G. Ramponi, C. M. Dobson, M. Stefani, *Nature* **2002**, 416, 507.
- [16] B. Caughey, P. T. Lansbury, *Annu. Rev. Neurosci.* **2003**, 26, 267.

- [17] F. Chiti, C. M. Dobson, *Annu. Rev. Biochem.* **2006**, 75, 333.
- [18] E. Katz, I. Willner, *Angew. Chem.* **2004**, 116, 6166; *Angew. Chem. Int. Ed.* **2004**, 43, 6042.
- [19] T. P. Knowles, A. W. Fitzpatrick, S. Meehan, H. R. Mott, M. Vendruscolo, C. M. Dobson, M. E. Welland, *Science* **2007**, 318, 1900.
- [20] G. Bhak, J. H. Lee, J. S. Hahn, S. R. Paik, *PLoS One* **2009**, 4, e4177.
- [21] J. H. Lee, G. Bhak, S. G. Lee, S. R. Paik, *Biophys. J.* **2008**, 95, L16.
- [22] G. Bhak, S. Lee, J. W. Park, S. Cho, S. R. Paik, *Biomaterials* **2010**, 31, 5986.
- [23] G. Bhak, Y. J. Choe, S. R. Paik, *BMB Rep.* **2009**, 42, 541.
- [24] J. F. Smith, T. P. Knowles, C. M. Dobson, C. E. Macphee, M. E. Welland, *Proc. Natl. Acad. Sci. USA* **2006**, 103, 15806.
- [25] V. N. Uversky, J. Li, A. L. Fink, *J. Biol. Chem.* **2001**, 276, 10737.
- [26] J. L. Gu, J. L. Shi, G. J. You, L. M. Xiong, S. X. Qian, Z. L. Hua, H. R. Chen, *Adv. Mater.* **2005**, 17, 557.
- [27] A. Kiesow, J. E. Morris, C. Radehaus, A. Heilmann, *J. Appl. Phys.* **2003**, 94, 6988.
- [28] S. Mann, *Nat. Mater.* **2009**, 8, 781.